Journal of Applied Electrochemistry (2007) 37:219–224
DOI 10.1007/s10800-006-9236-6

Selective area deposition of Tin–Nickel alloy coating – an alternative for decorative chromium plating

B. SUBRAMANIAN*, S. MOHAN and SOBHA JAYAKRISHNAN
Central Electrochemical Research Institute (CECRI), Karaikudi, 630006, Tamil Nadu, India
*(*author for correspondence, tel.: +91-4565-227555, fax: +91-4565-227713, e-mail: bsmanian@cecri.res.in)*

Received 12 April 2006; accepted in revised form 6 September 2006

Key words: corrosion resistance, selective area deposition, Sn–Ni alloy

Abstract

Sn–Ni alloy coatings on mild steel substrates produced by selective area deposition process with layer thickness of about 14 μm were investigated with regard to the structural and corrosion properties. X-ray diffraction analysis revealed that the selective area plated Sn–Ni alloy was heterogeneous and composed of NiSn, Ni_3Sn_2 and Ni_3Sn_4 phases. Uniform surface coverage of the substrate by granular morphology was observed from SEM and AFM. The alloy composition was determined by X-ray fluorescence (XRF). The corrosion protection performance of Sn–Ni alloy on mild steel was assessed using salt-water immersion and electrochemical corrosion tests. A sharp decrease in I_{corr} and high charge transfer resistance indicated improved corrosion resistant behavior of the selective area deposited Sn–Ni alloy.

1. Introduction

Electrodeposited chromium has high hardness, wear and corrosion resistance and reflectivity and has been applied to different industrial products such as automobiles [1, 2]. However, chromium (VI) electroplating processes produce large volumes of chromium-contaminated toxic waste, air pollution and water contamination which can result in significant induction of cytogenetic damage in electroplating workers [3] and genotoxic effects associated with occupational exposure [4, 5] to chromium.

Tin–nickel alloy is resistant to corrosion, resists tarnishing and retains its brightness. It has good contact and wear resistance. The Sn–Ni plating solution has a deep throw so that where there is a problem in plating chromium in deep recesses, tin–nickel alloy is an alternative. Tin–nickel alloy also has excellent frictional resistance and has the ability to retain an oil film on its surface. Because of these properties the alloy has found applications in engineering fields such as automotive breaking systems, heavy-duty switch gears and mixing valves. From this viewpoint, Sn–Ni plating is a good substitute for chromium plating [6]. Wear resistance of printed circuit boards was found to be superior when tin–nickel coating was included between copper and gold deposits [7].

Selective area deposition, also known as brush-plating, is a portable process for accurately applying plated deposits onto localized areas. It differs from traditional tank or bath plating in that the work piece is not immersed in a plating solution (electrolyte). Instead, the electrolyte is brought to the part to be plated and applied by a hand held anode or stylus, which incorporates an absorbent wrapping for applying the solution to the work piece (cathode). A DC power pack drives the electrochemical solution, depositing the desired material on the substrate. A schematic of the brush-plating process is shown in Figure 1. It offers portability, flexibility and high-quality deposits. The present work deals with the brush-plating of tin–nickel alloys on steel substrates and to study the influences of solution composition and operating parameters. The morphology, elemental composition and corrosion resistance of the alloy coating were also determined.

2. Experimental

The alloy coatings were brush-plated on mild steel (MS) substrates. The composition of the low carbon steel substrate used is shown in Table 1. In this work commercially available brush-plating equipment, Selectron power pack, USA, Model 150A-40V was utilized. The bath composition and bath parameters used for the alloy deposition are shown in Table 2. Solutions were prepared from reagent grade chemicals and distilled water. Mild steel specimens, $5 \times 2.5 \times 0.5$ cm, were

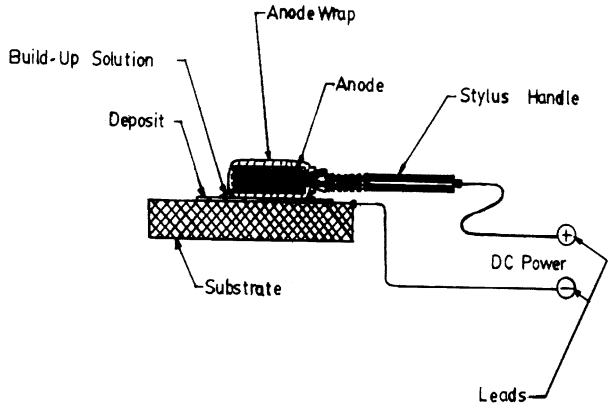

Fig. 1. Schematic of brush-plating process.

Table 1. Specified composition of carbon steel substrate

% C	% Mn	% S	% P	% Fe
0.063	0.23	0.03	0.011	Balance

Table 2. Optimized bath parameters for the brush-plating of Sn–Ni alloy

$SnCl_2 \cdot 2H_2O$	50 g l^{-1}
$NiCl_2 \cdot 6H_2O$	250 g l^{-1}
$NH_4 HF_2$	40 g l^{-1}
NH_3 (s.g – 0.88)	10 ml
PH	2.5
Bath temperature	28 °C (RT)
Plating voltage	2 V
Duration	30 min
Anode	Graphite stylus

polished mechanically and degreased with acetone. Following ultrasonic cleaning in acetone and washing in DI water the specimens were used for brush-plating. The deposit thickness was determined using a Mitutyo profilometer. A region of the mild steel substrate was masked before brush-plating. A stainless steel stylus with a diamond tip was drawn across the step from the substrate to the coating and both the vertical and horizontal motion of the stylus was amplified and recorded. The composition of the deposit was analyzed by HORIBA X ray analytical Microscope XGT 2000 with a Rh source at 20 KeV. Structural characterization of the deposit was carried out by XRD using an X'pert pro Philips X-ray diffractometer. Differential Thermal Analysis (DTA) measurements were carried out by STA 1000/15000 at a scanning rate of 20° min^{-1}. Surface morphological examinations were carried out using a Hitachi S 3000H Scanning Electron Microscope (SEM) and Molecular Imaging Atomic Force Microscope (AFM). The micro-hardness of the brush-plated samples was determined using a Micro hardness Testing Machine Leco DM 400 with a Vickers indenter and a load of 25 g. The corrosion resistance of the deposit was assessed by electrochemical polarization studies and AC Impedance measurement using a BAS IM6 Electrochemical analyzer. Experiments were carried out using the standard three-electrode configuration with saturated calomel as a reference electrode, a platinum foil as counter electrode and the sample as working electrode. The specimen (1.0 cm^2 exposed area) was immersed in the test solution of 3.5% w/v NaCl. Experiments were carried out at room temperature (28 °C).

3. Results and discussion

The brush-plated alloy samples were bent through an angle of 180° repeatedly as required by BS 5411 standards and no lifting and peeling was found which indicated good adhesion of the coatings to the mild steel substrates. Deposits with a Vickers hardness of 620 and 540 HV (25 g) were obtained for the as prepared and annealed Sn–Ni alloy which are comparable to that of chromium. The decrease in hardness for the annealed sample may be due to the increase in grain size observed for these films from XRD and SEM. A thickness of 14.2 μm was observed from Profilometric roughness and thickness measurement. This is in good agreement with the value of 14 μm obtained from the weight difference method. Figure 2 shows the DTA curve of the brush-plated Sn–Ni alloy. The base line was found to decrease with increasing temperature. The formation of NiSn and the stable compounds thereafter are presumed to occur up to about 600 °C. The endothermic peak at about 740 °C can be attributed to the melting of Ni_3Sn_4. It is evident that no fixed melting temperature existed for the alloy. The fusing temperature was neither the melting point of tin nor of nickel. Figure 3 shows the XRF spectrum of the sample. The L_β^1 and L_β^2 peaks for the Sn and K_α and K_β peaks appearing for Ni indicated that the Sn rays are less energetic than Ni. The chemical analysis of Figure 3 gives the composition as 65 tin and 35 nickel in weight percentage.

3.1. *XRD Analysis*

The X-ray diffractogram (XRD) for the brush-plated tin–nickel alloy as plated from the bath under optimized

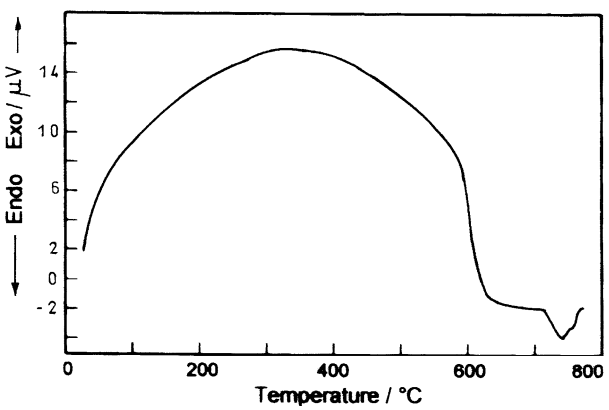

Fig. 2. DTA curve of the Sn–Ni alloy.

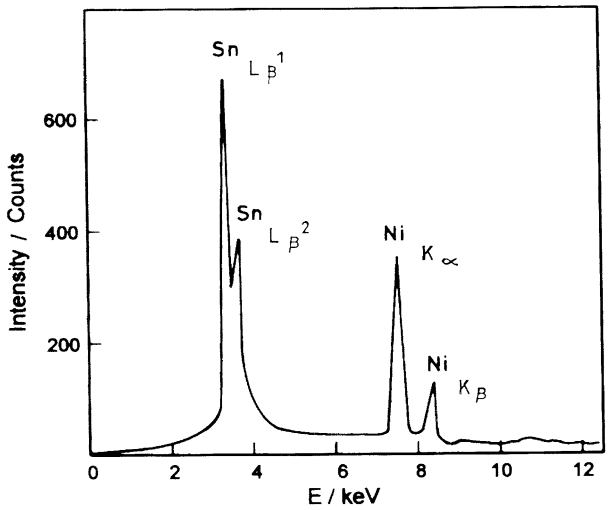

Fig. 3. XRF analysis of the as prepared Sn–Ni alloy film.

conditions is shown in Figure 4(a). Table 3 correlates the measured results in Figure 4(a, b) with the standard peaks from the JCPDS index cards. The data shows the observed interplanar distance, *d*' values are in good agreement with the standard, *d*' values of the corresponding phases. The presence of NiSn compound was confirmed although this phase is not found in the tin–nickel phase diagram (Figure 5) [8, 9]. The layer is thermodynamically unstable.

Figure 4(b) shows the XRD spectrum for the specimen heated to 400 °C and Table 3 shows the list of observed peaks and the JCPDS index. The annealing temperature was above the melting point of tin and much lower than that of nickel. The higher temperature enhances tin and nickel diffusion which, in turn, allows thermodynamically stable compounds to form. More stable compounds, Ni_3Sn_4 and Ni_3Sn_2 were formed. The structure and lattice parameters for these phases are indicated in Table 4. The crystallite size (*D*) of the films was calculated from the Scherrer's formula from the full width at half-maximum (β) of the peaks expressed in

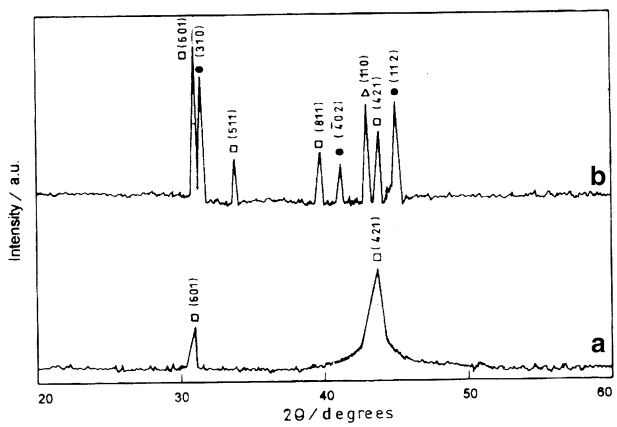

Fig. 4. X-ray diffractogram of Sn–Ni alloy film (a) as prepared (b) annealed □ – NiSn, • – Ni_3Sn_4, Δ – Ni_3Sn_2.

Table 3. Comparison of observed inter-planar distances and standard inter-planar distances of XRD pattern of brush-plated Sn–Ni alloy(annealed)

d – observed	*d* – standard	*h k l*	Relative intensity/%	Phase
2.884	2.886	(601)	100	NiSn
2.843	2.840	(310)	51.6	Ni_3Sn_4
2.647	2.649	(511)	21.6	NiSn
2.094	2.076	(110)	51.9	Ni_3Sn_2
2.058	2.047	(421)	46.6	NiSn
2.013	2.033	(112)	48.9	Ni_3Sn_4

radians

$$D = 0.94\lambda/\beta \cos\theta \quad (1)$$

where β is the FWHM calculated from the (421) plane. The crystallite size was calculated from line broadening, under the simple assumption that the line broadening is caused by the crystallite size alone [10]. The average crystallite sizes were found to be 0.7 (601) and 0.3 (421) μm for the as prepared NiSn layers and 1.4 (601) and 1.5 (421) μm for the annealed NiSn layers on mild steel substrates. The increase in crystallite size may be due to agglomeration of grains during annealing.

3.2. *Surface morphology*

Examination of the surface morphology by SEM showed that the as prepared and annealed Sn–Ni alloy brush-plated at the plating voltage of 2 V (Figure 6a, b), were compact and consisted of fine grains covering the whole substrate surface.

The average size of the grains was determined to be 1.0 and 1.5 μm by Cottrell's method [11] from SEM for the as prepared and annealed samples, respectively. The deposits were found to be microcraked and it is known that such cracks form during brush-plating when the tensile stress exceeds the cohesive strength of the deposit.

Surface characterization of the brush-plated Sn–Ni alloy sample was carried out using atomic force microscopy (AFM). The advantage of AFM is its capacity to probe minute details related to the individual grains and inter-grain regions. A representative AFM picture scanned over an area of 1 × 1 μm of the annealed Sn–Ni alloy sample prepared under optimized conditions is shown in Figure 7. The deposit consists of many small spherical particles which are characteristic of brush-plated Sn–Ni coatings.

Table 4. Crystallite size and lattice parameters of Sn–Ni alloy

Phase	JCPDS Card No.	Lattice parameters		
		a/Å	*b*/Å	*c*/Å
NiSn	26-1289	24.54	5.400	4.051
Ni_3Sn_4	04-0846	12.22	4.062	5.167
Ni_3Sn_2	08-0430	4.14	–	5.106

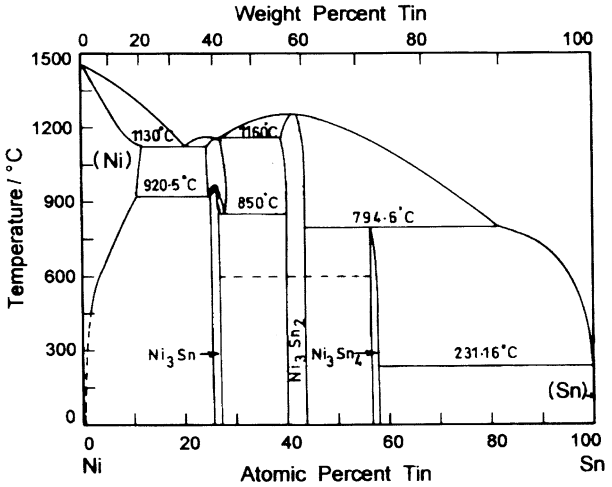

Fig. 5. Phase diagram of Tin and Nickel.

3.3. *Potentiodynamic polarization studies*

The potentiodynamic polarization curves obtained for the mild steel (substrate), brush-plated Sn, as prepared Sn–Ni alloy on mild steel and the annealed sample in 3.5% w/v NaCl electrolyte are presented in Figure 8. The E_{corr} and I_{corr} values were calculated using the Tafel extrapolation method as given in Table 5. There is an appreciable increase in corrosion resistance for the annealed Sn–Ni alloy on mild steel substrate compared to tin on mild steel, chromium on mild steel, as prepared alloy and bare mild steel substrate which may be due to passive film formation on the surface [12]. E_{corr} and I_{corr}

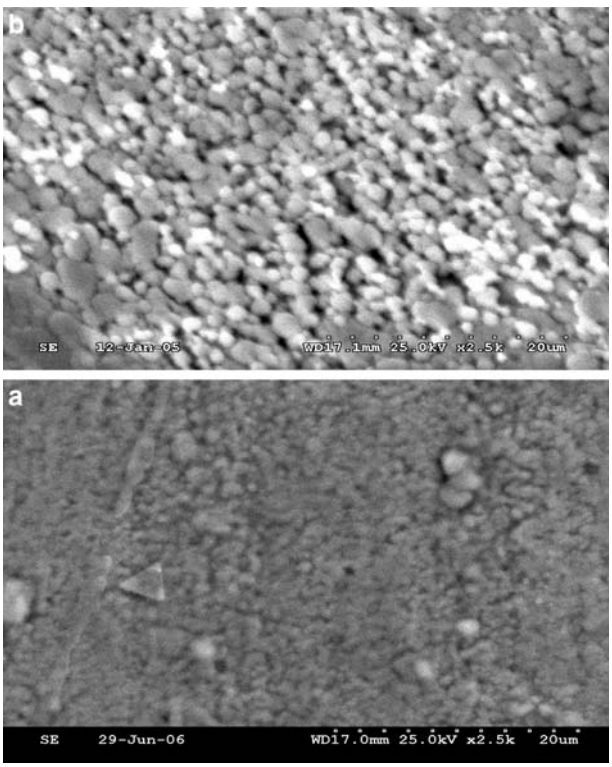

Fig. 6. Scanning electron micrograph of (a) as prepared (b) annealed Sn–Ni alloy film.

Table 5. Corrosion parameters obtained from polarization studies in 3.5% w/v NaCl

Sample	E_{Corr}/Vs SCE/mV	ba/V dec^{-1}	bc/V dec^{-1}	I_{Corr}/A cm^{-2}
MS panel	−0.680	0.118	−0.196	1.26×10^{-4}
Sn on MS	−0.542	0.177	−0.201	1.80×10^{-5}
Cr on MS	−0.504	0.128	−0.226	1.25×10^{-5}
Sn–Ni alloy on MS (as prepared)	−0.527	0.118	−0.226	0.57×10^{-5}
Sn –Ni alloy on MS (annealed)	−0.485	0.121	−0.155	7.43×10^{-6}

values improve (a less negative value of E_{corr} and lower value of I_{corr} signifies an improvement in corrosion resistance) for the annealed Sn–Ni alloy on mild steel substrate. The E_{corr} values are shifted to near the equilibrium value of the Sn–Ni alloy system, which indicates a reduction in corrosion.

3.4. *Electrochemical impedance*

The electrochemical impedance spectra of brush-plated Sn–Ni alloy system were measured with the same three-electrode assembly as used for the potentiodynamic polarization experiments. Impedance measurements were made at open circuit potential (OCP) applying an AC signal of 10 mV in the frequency range of 10 Hz to 1 MHz. The impedance results obtained from Nyquist plots for the samples used for corrosion tests in 3.5% w/v NaCl solution are shown in Table 6 and Figure 9.

The charge transfer resistance R_{ct} can be related to I_{corr} [13]

$$R_{ct} = b_a \times b_c / 2.3\,(b_a + b_a) I_{corr} \quad (2)$$

where R_{ct} is charge transfer resistance, b_a and b_c are anodic and cathodic Tafel slopes.

The double layer capacitance C_{dl} value is obtained from the frequency at which Z imaginary is maximum [13]

$$\omega\left(Z_{(im)}\,\max\right) = 1/C_{dl}R_{ct} \quad (3)$$

The increased R_{ct} values and decreased C_{dl} values for the annealed Sn–Ni alloy clearly confirm the better corrosion resistance of these systems compared to as prepared alloy, tin on mild steel, chromium on mild steel and bare mild steel substrate. Also a more pronounced semicircular region is observed in the case of the annealed Sn–Ni alloy sample indicating that the system has good corrosion resistance as observed from the high frequency region of the impedance spectra.

The corrosion resistance of the Sn–Ni alloy deposit was also assessed by salt water immersion testing. The deposits were dipped in a 3.5% w/v NaCl solution at room temperature. The appearance of the surface after immersion in the solution for different duration is presented in Table 7. Comparing the corrosion resistance of the blank mild steel panel and

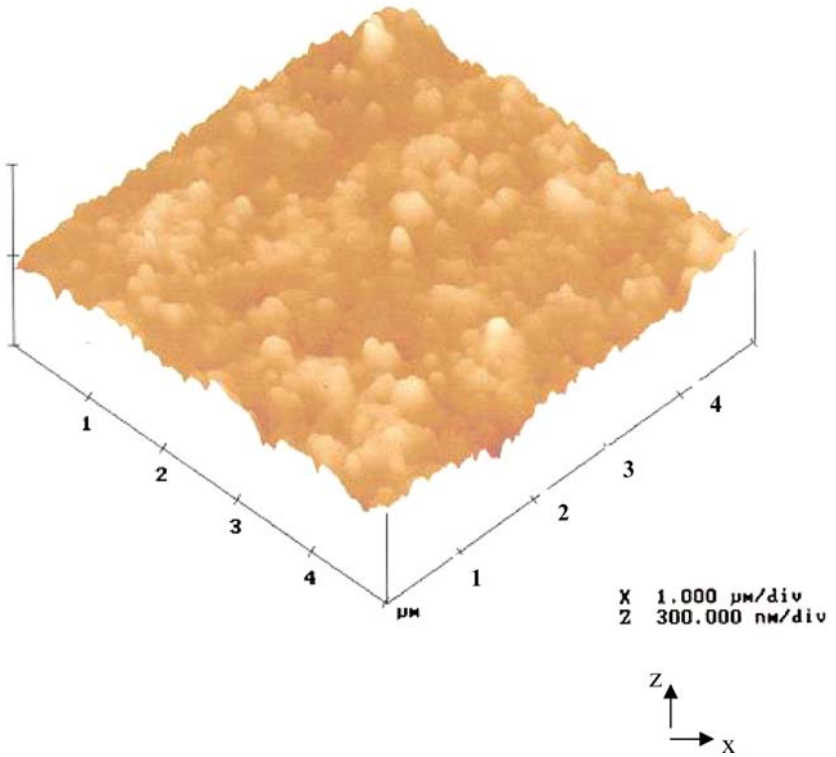

Fig. 7. AFM images (scan size 5×5 μm) showing the topography of annealed Sn–Ni alloy film on mild steel sample.

brush-plated tin on mild steel, chromium on mild steel and the as prepared Sn–Ni alloy, the annealed Sn–Ni alloy deposit appears to be more corrosion resistant.

4. Conclusions

Adherent, smooth, bright Sn–Ni alloy deposits were brush-plated successfully onto low carbon steel substrates from chloride bath. The brush-plated Sn–Ni alloy films are heterogeneous systems comprising intermetallic compounds (NiSn, Ni_3Sn_4, Ni_3Sn_2). Uniform coverage of spherical nodular morphology is observed from microstructure analyses. The annealed Sn–Ni alloy deposit obtained from the bath composition and bath

Table 6. Corrosion parameters obtained from impedance measurements by Nyquist plots

Sample	OCP/V	R_{ct}/Ohm cm^2	C_{dl}/farads cm^{-2}
MS Panel	−0.655	93.8	5.63×10^{-3}
Sn on MS	−0.506	1032.8	1.40×10^{-4}
Cr on MS	−0.478	1100.7	0.89×10^{-4}
Sn –Ni alloy on MS (as prepared)	−0.483	1382.4	0.75×10^{-4}
Sn –Ni alloy on MS (annealed)	−0.468	1519.17	9.56×10^{-5}

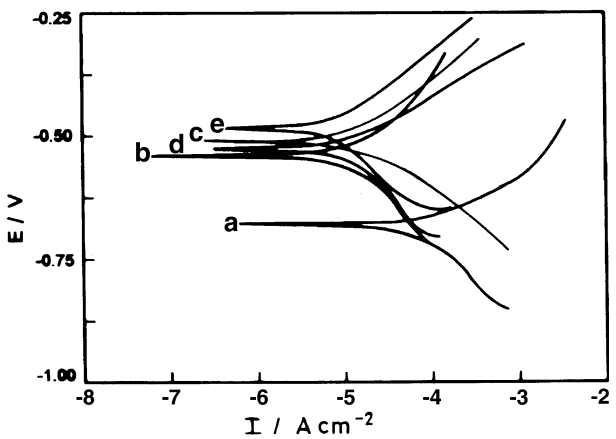

Fig. 8. Polarization studies of (a) blank MS (b) Sn on MS (c) Cr on MS (d) as prepared Sn–Ni alloy film (e) annealed Sn–Ni alloy film on MS in 3.5% w/v NaCl.

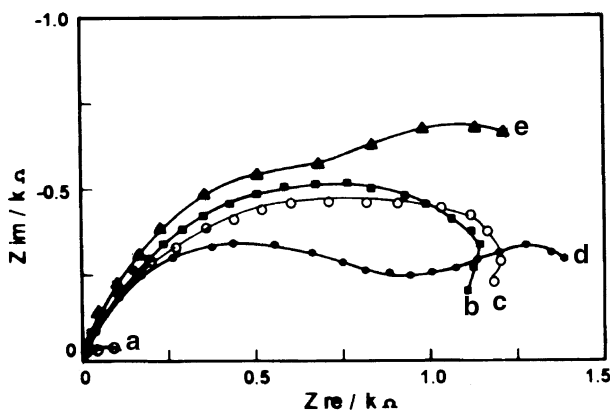

Fig. 9. Nyquist plots for corrosion measurements of (a) blank MS (b) Sn on MS (c) Cr on MS (d) as prepared Sn–Ni alloy film (e) annealed Sn–Ni alloy film on MS in 3.5% w/v NaCl.

Table 7. Results of tarnishing/rusting level after salt water dipping

Sample	8 h	1 day	4 days	7days
Blank MS	10%	60%	100%	100%
Sn on MS	No	No	25%	30%
Cr on MS	No	No	3%	10%
Sn–Ni alloy on MS (as prepared)	No	No	2%	5%
Sn–Ni alloy on MS (annealed)	No	No	No	3%

parameters given in Table 2 demonstrated excellent corrosion protective performance.

References

1. S.S. Abd. El Rehim, M.A.M Ibrahim and M.M. Dankeria, *Trans. Inst. Met. Finish.* **80** (2002) 29.
2. AESF Features, ‚Chromium is prominent on 2000 auto designs', *Plating Surf. Finish.* **87** (2000) 10.
3. F. Wn, W. Wn, H. Kuo, C. Lin, R. Wang and J. Lai, *Sci. Total Environ.* **279** (2001) 21.
4. A. Vaglenov, M. Nosko, R. Georgieva, E. Carbonell, A. Creus and R. Marcos, *Mater Res.* **446** (1999) 23.
5. H. Xu, R. Akid and G. Brumpton, *Trans. Inst. Met. Finish.* **82** (2004) 18.
6. T. Kobayashi, H. Kanematsu, M. Yoshitake and T. Oki, *Trans. Inst. Met. Finish.* **80** (2002) 194.
7. S.K. Jalota, *Met Finish* **100** (2002) 307.
8. M. Jordan, *The Electrodeposition of Tin and 95 Alloys* (Engen G.Leuze Publishers, Saulgau, Germany, 1995), pp. 122.
9. ASTM International, Binary Alloy Phase Diagram (Update version 1.0) (ASM International, Materials Park, OH, 1998), 2nd edition.
10. M. Koch and U. Eberbach, *Surf. Eng.* **13** (1997) 157.
11. A. Cottrell, *Introduction to Metallurgy* (Arnold, London, 1975), pp. 173.
12. S.A.M. Refaey, F. Taha and T.H.A. Hasanin, *Appl. Surf. Sci.* **227** (2004) 416.
13. G. Venketachari, *Corr. Bull.* **2** (1982) 14.